High-K bands in the ^{166}Yb region

J.R.B. Oliveira,* S. Frauendorf,† M.A. Deleplanque, B. Cederwall,
R.M. Diamond, A.O. Macchiavelli, F.S. Stephens, and J. Burde‡
Nuclear Science Division, Lawrence Berkeley Laboratory, 1 Cyclotron Rd., Berkeley, California 94720

J.E. Draper, C. Duyar, and E. Rubel
University of California, Davis, California 95616

J.A. Becker, E.A. Henry, M.J. Brinkman, A. Kuhnert, M.A. Stoyer, and T.F. Wang
Lawrence Livermore National Laboratory, Livermore, California 94550
(Received 3 February 1994)

High-K bands have been observed in the ^{166,167,168}Yb isotopes following the ^{124}Sn(^{48}Ca,$xn\gamma$) reaction. The $\nu h_{11/2}$ band in ^{167}Yb has been extended to higher spins. The high-K bands in the even-even isotopes were observed for the first time and show very high $B(M1)/B(E2)$ ratios. Configuration assignments for the new bands are proposed. The results are interpreted within the tilted cranking model.

PACS number(s): 21.60.Cs, 21.10.Re, 27.70.+q

I. INTRODUCTION

The recent development of the "tilted axis cranking" (TAC) model [1,2] has revived the interest in the signature-degenerate $\Delta I = 1$ rotational bands. In that semiclassical model, the axis of rotation is no longer considered to coincide with one of the principal axes of the nuclear quadrupole deformation, but to be parallel to the total angular momentum vector. As a consequence, the intrinsic signature is undefined. In this case no energy staggering should be expected between odd and even spin states. The Yb region around mass 166 presents some of the best normal-deformed axially symmetric rotors known, and is therefore suitable for the observation of "tilted bands," as they are now called, without the complications of β- or γ-soft nuclear systems. On the other hand, tilted bands are rare in that nuclide region. The only high-Ω orbitals available are the $\nu[505]11/2^-$ from the $h_{11/2}$ neutron subshell, the $\pi[404]7/2^+$ ($g_{7/2}$), and the $\pi[523]7/2^-$ from the $h_{11/2}$ proton subshell. The last two orbitals are known to couple to a $I^\pi = 7^-$ bandhead state in some Er and Yb isotopes. High-Ω orbitals are necessary to boost high components of angular momentum along the symmetry axis (called K in this paper for simplicity). Another characteristic feature of most high-K bands is the appearance of strong $M1$ transitions. The present work reports the observation of bands with those characteristics in ^{167}Yb, ^{166}Yb, and ^{168}Yb. Part of the band in ^{167}Yb had been previously observed, and had been assigned the $\nu h_{11/2}$ configuration ($[505]11/2^-$). The other two bands were observed for the first time. For them we propose the $\pi([404]7/2 \otimes [523]7/2)$ proton configuration coupled to two distinct neutron configurations, $\nu[AB]$ and $\nu[AE]$ for ^{166}Yb and ^{168}Yb, respectively, where A and B are the first and second positive parity quasiparticle excitations (from the $i_{13/2}$ subshell), and E is the first negative parity quasiparticle excitation (from [523]5/2 and [521]1/2 parentage). These assignments give slightly better agreement with experimental data than the more simple $\nu[h_{11/2} \otimes i_{13/2}]$ configuration. However, the present data do not distinguish unambiguously between the two.

II. EXPERIMENTAL MEASUREMENTS AND RESULTS

The high-spin states of $^{165-168}$Yb were studied with the High Energy Resolution Array (HERA) at the 88-Inch Cyclotron of the Lawrence Berkeley Laboratory. HERA consisted of 20 Compton-suppressed germanium detectors and an inner ball of 40 BGO (bismuth germanate) detectors. The high-spin states were populated in the reaction ^{124}Sn(^{48}Ca,xn) at 210, 220, and 225 MeV. A stack of three self-supporting ^{124}Sn (97%) targets with ≈ 0.5 mg/cm^2 each separated by 0.5 mm gaps was used. About 420, 570, and 166×10^6 coincidence events [$\approx 80\%$ high fold ($k > 11$) doubles and $\approx 20\%$ triples] were recorded at each beam energy respectively. From the 210 MeV data, 650×10^6 counts were accumulated into a symmetrized $E\gamma \times E\gamma$ matrix with fold $k > 17$ and sum $H > 13$ MeV in the inner ball detectors. From the 220 and 225 MeV data two matrices were sorted at each beam energy, one with requirements of total fold (Ge + BGO) $15 < k < 25$, and total sum $13 < H(\text{MeV}) < 26$ (with 770 and 570×10^6 counts, respectively) and another

*Present address: Universidade de São Paulo, São Paulo, SP, 01498, C.P. 20516, Brazil.
†Present address: Institut für Kern und Hadronen Physik, FZ-Rossendorf, PF.19 0-8051 Dresden, Germany.
‡Present address: The Racah Institute for Physics, The Hebrew University, Jerusalem, Israel.

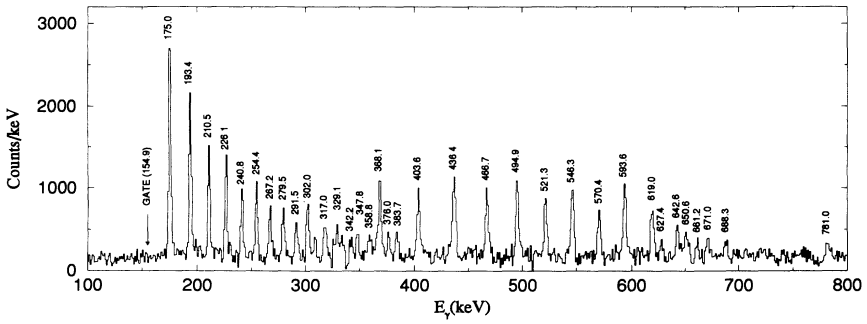

FIG. 1. Added spectra in coincidence with the 155 keV γ ray (^{167}Yb) from all the five matrices referred to in the text.

with $k > 24$, $H > 7$ MeV (with 227 and 154×10^6 counts, respectively).

Figures 1, 2, and 3 show coincidence spectra of energy gates on members of bands observed from those matrices. These bands show the characteristic pattern of high-K rotational bands, i.e., a sequence of regularly spaced lower energy transitions with no staggering, and higher energy crossover transitions. The crossover transitions are very weak in the cases of Figs. 2 and 3. Some of the indicated crossovers can only be confirmed in summed coincidence spectra of several energy gates, and in sums of double-gated spectra from three- and higher-fold Ge coincidences (Fig. 4). It was not possible to determine the decay paths connecting those bands with other lower lying states in the respective nuclei. This is due to the long half-life of the $11/2^-$ bandhead of the $\nu h_{11/2}$ band in ^{167}Yb (about 180 ns [3]), and probably to the same reason (long "bandhead" lifetimes) for the other bands, assigned here to ^{166}Yb and ^{168}Yb. In addition, such bands represent roughly 1% and 0.5% of the respective channel yields; i.e., they are very weakly populated structures. The $\nu h_{11/2}$ band in ^{167}Yb is populated with about 7% of the channel yield. We believe that the main reason why it is possible to observe such weakly populated structures, which supposedly lie at high excitation energy, is their high angular momentum component K along the symmetry axis. A high-K structure is not likely to deexcite to the other lower lying low-K structures due to K forbiddeness. Another reason is that most of the intensity of these bands goes through the dipole transitions, which are in an energy range of low density of $E2$ transitions from the stronger structures in the spectrum. Although some members of the respective ground state bands seem to be present in the spectra of Figs. 2 and 3, this cannot be considered as very good evidence for the channel assignments since those transitions are among the most intense in the corresponding sets of data, and their intensity is therefore very sensitive to changes in background subtraction.

The assignment of each band to the corresponding evaporation channel is based on the fold and sum-energy distributions associated with the in-band γ rays. Table I shows the ratio between in-beam γ-ray coincidence intensities from the two different sets of k and H requirements at a beam energy of 225 MeV, i.e.,

$$R = \frac{I_\gamma(i, f, 15 < k < 25, 13 < H < 26)}{I_\gamma(i, f, k > 24, H > 7)},$$

where $I_\gamma(i, f, k, H)$ is the coincidence intensity between γ rays from states i and f for a given condition on fold (k) and sum energy (H). As can be seen from that table, the ratio obtained for known coincident transitions is very sensitive to the number of neutrons of the respective evaporation residue. This ratio shows also very little sensitivity, if any, to the spin of the highest state of the decay path defined by the coincident transitions. We rely on this table to assign the band of Fig. 2 to the ^{166}Yb nucleus. The assignment of the band of Fig. 3 to ^{168}Yb is based on the fact that it is only observed on the 210 MeV data set, where the ^{168}Yb is by far the strongest channel. The ^{167}Yb transitions are observed with about the same intensity in both the 210 MeV matrix and in the $15 < k < 25$, $13 < H$(MeV)< 26 matrix at 225 MeV.

Figure 5 presents the level schemes for the high-K bands observed in the present work. They are generally consistent with the coincidence intensity between the transitions and sum-energy relationships between paral-

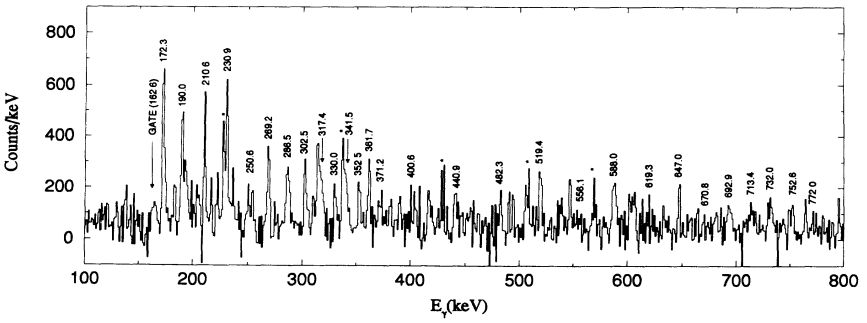

FIG. 2. Added spectra in coincidence with the 162 keV γ ray (^{166}Yb) from the $15 < k < 25$, $13 < H$(MeV)< 26 at 225 and 220 MeV matrices. Transitions marked with an asterisk belong to the ground state band of ^{166}Yb.

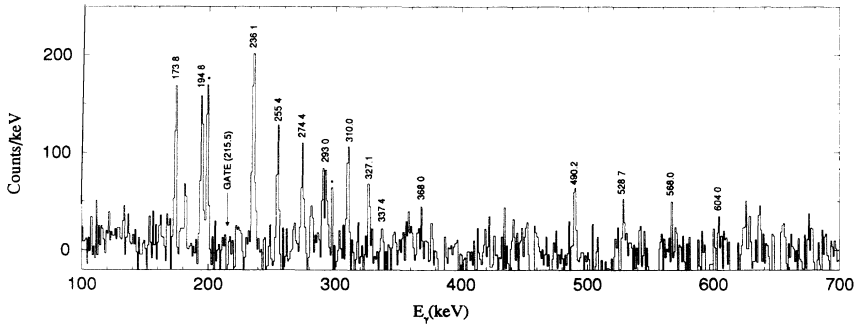

FIG. 3. Spectrum in coincidence with the 215 keV γ ray (^{168}Yb) from the $k > 17$, $H > 13$ MeV at 210 MeV matrix. Transitions marked with an asterisk belong to the ground state band of ^{168}Yb.

lel gamma-ray paths. The intensity of the 251 keV line (^{166}Yb) seems to be significantly below the average trend of the $\Delta I = 1$ transitions both in Figs. 2 and 4. This is not an effect of background subtraction since there is not a strong line with that energy in the background spectrum. Nevertheless, the scheme of Fig. 5(b) is the one that provided the best overall consistency with the data. The spins (I) of the "bandheads" in ^{166,168}Yb were not determined. The $\nu h_{11/2}$ band in ^{167}Yb was previously known from $(\alpha, 3n)$ [4] studies up to spin $(21/2^-)$ (the bandhead state $11/2^-$, with an excitation energy of 571 keV and lifetime of $\approx$ 180 ns was known from ^{167}Lu decay studies [3,5]). We added several higher lying transitions, and we disagree as to the existence of the 228.6 keV and the 454.0 gamma rays, which were tentatively assigned to the $(23/2) \rightarrow (21/2)$ and $(23/2) \rightarrow (19/2)$ transitions in Ref. [4]. The other bands were observed for the first time in the present work. The intensity pattern indicates that there is very little, if any, decay out of the band other than from the lowest lying state observed in each band. For that reason one could refer to those states as bandheads, although they may not be really so. Linking transitions to other states were not observed; therefore the relative excitation from the "bandhead" states to the ground state is not known. We expect it to be high (above 2 MeV) since the structures are very weakly populated.

From the branching ratio $I_\gamma(M1)/I_\gamma(E2)$ on each level it is possible to extract the reduced transition probability ratio $B(M1)/B(E2)$ from the formula (γ-ray energies in MeV)

$$\frac{B(M1)}{B(E2)}[(\mu_N)^2/(e^2b^2)] = 0.693 \times \frac{E_\gamma^5(E2)}{E_\gamma^3(M1)} \frac{I_\gamma(M1)}{I_\gamma(E2)}.$$

The results are presented in Figs. 6, 7, and 8. For the even-even nuclei, since the spins are not known, the plot is done as a function of the rotational frequency rather than as a function of spin. The large uncertainties, particularly for the even-even isotopes, are due to the low statistics of the weak $E2$ transitions. The experimental points are calculated assuming a multipolarity mixing ratio $I_\gamma(E2)/I_\gamma(M1) = \delta^2 = 0$ for the $\Delta I = 1$ transitions. Our directional correlation (DCO) measurements for the $\nu h_{11/2}$ band in ^{167}Yb (Fig. 9) are consistent with a small mixing ratio ($\leq$ 10%). Due to the low statistics of this kind of measurement no attempt was made to measure the DCO ratios for the other weaker bands in the even-even nuclei. The assumption of $\Delta I = 1$, $M1$ $(+E2)$ transitions and $\Delta I = 2$, $E2$ crossovers is based on the close resemblance between the three level schemes (Fig. 5).

Figure 10 shows the dynamic moment of inertia of the high-K bands of the present investigation as a function of rotational frequency. The two $i_{13/2}$ quasineutron band (AB) in ^{166}Yb is also shown for comparison. The dynamic moment of inertia ($\mathcal{J}^{(2)}$) is calculated from each adjacent pair of in-band γ-ray transitions from

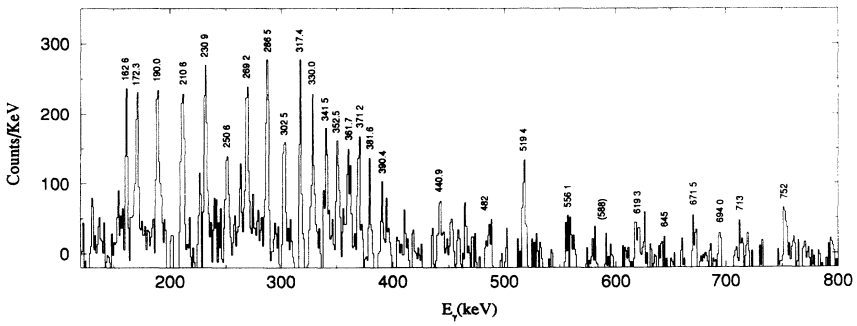

FIG. 4. Sum of doubled-gated spectra on all dipole members of the ^{166}Yb band [$15 < k < 25$, $13 < H$(MeV)< 26 at 225 MeV]. The background spectrum was chosen to be the total projection of the cube, normalized to give zero total counts in the subtracted spectrum. The 588 keV line does not appear because there is a very large peak in the total projection with that energy.

TABLE I. Ratio between coincidence intensities from two k and H conditions, as defined in the text. $E\gamma(i)$ and $E\gamma(f)$ are the coincident γ rays from the initial and final states with spin $I(i)$ and $I(f)$, respectively. The corresponding evaporation residue (channel) is indicated, where known. New assignments are in parentheses.

$E\gamma(i)$ (keV)	$E\gamma(f)$ (keV)	$I(i)(\hbar)$	$I(f)(\hbar)$	Ratio	Channel
298	199	6	4	0.13(1)	^{168}Yb
552	298	14	6	0.127(5)	^{168}Yb
174	155	15/2	13/2	0.85(7)	^{167}Yb
193	155	17/2	13/2	0.88(9)	^{167}Yb
210	155	19/2	13/2	0.8(1)	^{167}Yb
313	222	21/2	17/2	0.87(1)	^{167}Yb
743	222	49/2	17/2	0.86(2)	^{167}Yb
172	162	$(I+2)$	$(I+1)$	2.6(6)	(^{166}Yb)
269	162	$(I+7)$	$(I+1)$	1.8(8)	(^{166}Yb)
337	228	6	4	2.50(4)	^{166}Yb
666	228	22	4	2.54(5)	^{166}Yb
322	206	21/2	17/2	7.2(5)	^{165}Yb
429	322	25/2	21/2	7.77(15)	^{165}Yb
524	322	29/2	21/2	7.52(16)	^{165}Yb

$$\mathcal{J}^{(2)} = (\Delta I)^2\hbar^2/\Delta E_\gamma(\Delta I),$$

where $\Delta I = 1$ for the high-K bands and $\Delta I = 2$ for the AB band, and E_γ are the energies of the transitions. We assume that the frequency is $\hbar\omega = E_\gamma/\Delta I$ where the energy of the lower transition of the pair is used. No signature splitting is observed in any of the three bands (except possibly at the highest frequencies) of the present investigation which is characteristic of high K.

III. DISCUSSION

As mentioned in the Introduction, high-K bands are not commonly observed in this mass region. Most of the neutron orbits near the Fermi surface have $\Omega = 5/2$ or less and do not yield high angular momentum projections onto the symmetry axis. The only exception is the [505]11/2 holelike state from the top of the $h_{11/2}$ subshell, which is, however, not very near to the Fermi surface except for larger β deformation. Bands built on this state are known in a number of Er, Dy, Gd, and Sm odd-N isotopes, and in ^{149}Nd and ^{167}Yb. The proton states are usually not active due to the $Z = 70$ gap. A $I^\pi = K^\pi = 7^-$ state can be formed by combining the [523]7/2 with the [404]7/2 proton states. Bands built on this state are known in a few Er isotopes and in ^{170}Yb.

The high-K band in ^{167}Yb has been assigned the ν[505]11/2 configuration [3,4]. Our measurement of the $B(M1)/B(E2)$ ratios for this band are in reasonable agreement with what can be expected from such a configuration. Also, the part of the band extended to higher-

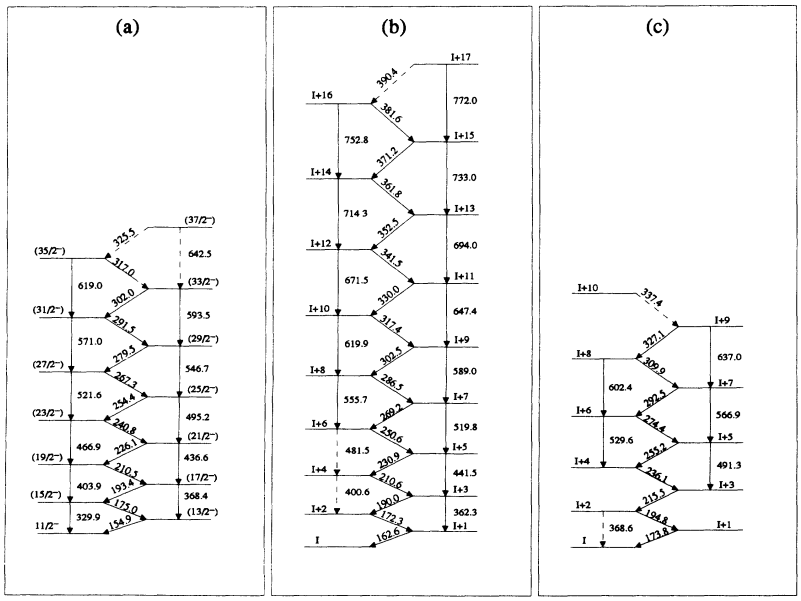

FIG. 5. Level schemes for the $\Delta I = 1$ bands in (a) ^{167}Yb, (b) ^{166}Yb, and (c) ^{168}Yb.

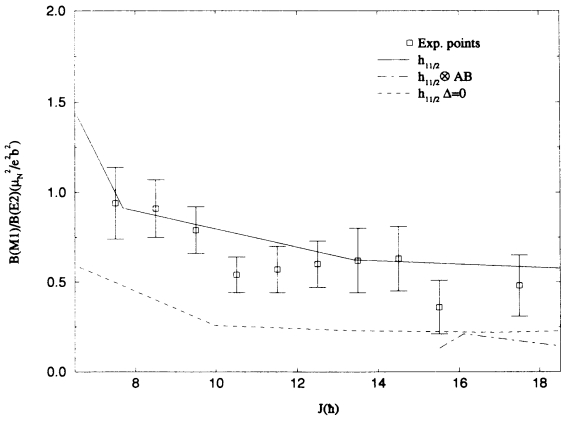

FIG. 6. Experimental and calculated $B(M1)/B(E2)$ ratios as a function of the total spin (J) for the ^{167}Yb band. The solid and dot-dashed lines are for the $\nu h_{11/2}$ and $\nu h_{11/2}AB$ configurations, respectively, as calculated from the TAC model. The dashed line is for $\nu h_{11/2}$ with $\Delta_\nu = 0$.

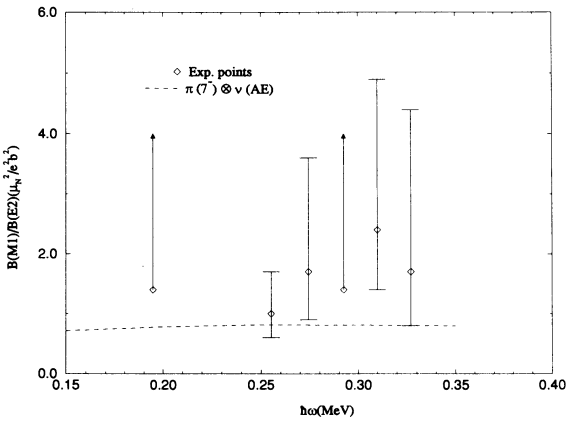

FIG. 8. Experimental and calculated $B(M1)/B(E2)$ ratios as a function of rotational frequency for the ^{168}Yb band ($\delta = 0$ assumed). The solid curve is calculated from the tilted model for the $\pi[7^-] \otimes \nu[AE]$ configuration.

spin states is consistent with an increase in alignment from a very smooth AB crossing Ref. [6]. The AB crossing is not blocked for any negative parity single quasiparticle configuration in contrast to the positive parity ones. We therefore agree with the aforementioned assignment.

For the bands in the even-even isotopes $^{166-168}$ Yb we considered various possible assignments. The coupling of the $h_{11/2}$ quasineutron with the first $i_{13/2}$ quasineutron A would yield the least excited two quasiparticle band with a relatively high K. The AB crossing would be blocked for such a configuration. No backbend is observed around the AB crossing frequency (0.25 MeV) in the ^{166}Yb band [7] and no upbend in the ^{168}Yb band [8]. The $\nu[h_{11/2} \otimes i_{13/2}]$ (or simply $\nu[h_{11/2}A]$) assignment seemed therefore attractive for both bands. However, calculations of the $B(M1)/B(E2)$ ratio for that configuration underestimate by at least a factor of 2 the experimental results obtained (Fig. 7). This is due to a partial cancellation of the magnetic moment perpendicular to the spin axis from the "deformation-aligned" (DAL) $h_{11/2}$ quasineutron and the more "rotation-aligned" (RAL) quasineutron $i_{13/2}$. In addition, there is evidence for an upbend in the dynamic moment of inertia at low fre-

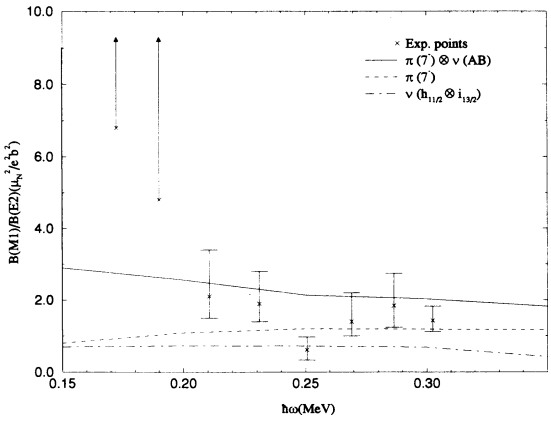

FIG. 7. Experimental and calculated $B(M1)/B(E2)$ ratios as a function of rotational frequency for the ^{166}Yb band ($\delta = 0$ assumed). The solid, dashed, and dot-dashed lines are for the $\pi[7^-] \otimes \nu[AB]$, $\pi[7^-]$, and $\nu[h_{11/2} \otimes A]$ configurations, respectively, as calculated from the TAC model.

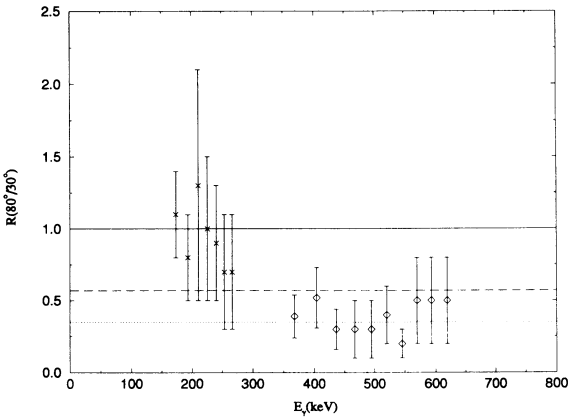

FIG. 9. Directional correlation measurements (DCO) for the γ-ray transitions of the $\nu h_{11/2}$ band in ^{167}Yb. The ratio of coincidence intensities indicated, $R(80°/30°)$, is given by the intensity of the γ rays (of energy E_γ) detected at $\approx 80°$ or (180–80)° in coincidence with the 155 keV γ ray detected at $\approx 30°$ or (180–30)° divided by the intensity of the γ rays (of energy E_γ) detected at $\approx 30°$ or (180–30)° in coincidence with the 155 keV γ ray detected at $\approx 80°$ or (180–80)° (the angles are measured to the beam direction). The solid line is the expected value for transitions of the same multipolarity as that of the 155 keV transition. The 155 keV transition is presumably of $M1+\delta^2 E2$ multipolarity. With this hypothesis, the dashed and dotted lines would be the expected values for pure $E2$ transitions in coincidence with the 155 keV transition for $\delta^2 = 0$ and $\delta^2 = 0.1$, respectively. The expected values were calculated specifically for the HERA system. The data points marked with crosses and diamonds were tentatively assigned to $M1 + \delta^2 E2$ and $E2$ multipolarities, respectively, [see Fig. 5(a)].

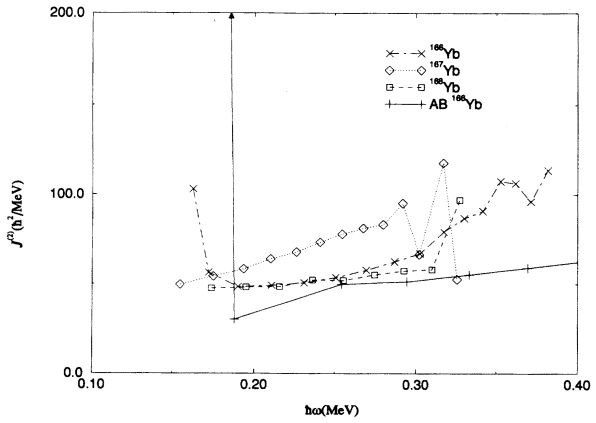

FIG. 10. Experimental dynamic moments of inertia as a function of rotational frequency for the $^{166-168}$Yb high-K bands. Diamonds ^{167}Yb, ×'s ^{166}Yb, squares ^{168}Yb (the error bars are about equal to or smaller than the symbol sizes). The AB (or s) band of ^{166}Yb (K=0) is also shown for comparison (+). The first data point (indicated by an arrow) is off scale at $\hbar\omega = 0.182$ MeV, $\mathcal{J}^{(2)} = 387\hbar^2/\mathrm{MeV}$. The lines are traced to guide the eye only.

quency for the ^{166}Yb band (Fig. 10). Such an upbend could not be explained with the $\nu[h_{11/2}A]$ assignment.

This situation led us to search for alternative assignments for those bands. One possibility is the quasiproton configuration $\pi([523]7/2 \otimes [404]7/2)$ which is known to form the $I^\pi = 7^-$ in some Er and Yb isotopes. For simplicity we will refer to this configuration as $\pi[7^-]$. The calculated $B(M1)/B(E2)$ branching ratio for this high-K proton configuration is close to 1 for a wide frequency range, and therefore closer to the experimental values. A disadvantage of this assignment is that the first neutron crossing (AB) is not blocked and should be present. A rather weak interaction would be expected for this crossing in ^{166}Yb [7] and a strong interaction in ^{168}Yb [8] as happens in the crossing of the ground state band with the s band ($\nu[AB]$) of the respective nuclei. No crossings with these characteristics are present in the bands of this work. We therefore propose that the band seen experimentally is the $\pi[7^-]$ coupled to the first "aligned" pair of $i_{13/2}$ quasineutrons ($\nu[AB]$). For this configuration the moment of inertia should be smooth down to the spin where it crosses with the $\pi[7^-]$. This is an analog case to the crossing of the s with the g band of ^{166}Yb seen in Fig. 10. The upper branch of the crossing occurs at $\omega \approx 0.18$ MeV in the s band whereas it is seen at $\omega \approx 0.16$ MeV in the high-K band. We believe this difference is not incompatible with the proposed assignment since $\mathcal{J}^{(2)}$ is a quantity very sensitive to small disturbances. For this configuration strong magnetic transitions are expected since the aligned neutrons contribute to the already large magnetic moment perpendicular to the spin axis from the high-K proton configuration. This is consistent with the very large $M1/E2$ branching ratios observed down to the lowest frequencies (Fig. 7).

In ^{168}Yb, however, no upbend is seen in the dynamic moment of inertia plot down to the lowest observed transitions. For this band we considered the same proton configuration coupled to the first negative parity neutron configuration (AE) which has the AB crossing blocked. The $M1/E2$ branching ratios are not as large as in the $\pi[7^-]\otimes\nu[AB]$ configuration, but are still rather large. We would like to point out that the AB crossing should have a large interaction in ^{168}Yb, which would result in a rise of the dynamic moment of inertia over a wide frequency range in contradiction with experiment (Fig. 10).

If these assignments are correct, though, we should explain why the pure proton configuration is not seen in either of the two isotopes. Both bands, particularly $\pi[7^-] \otimes \nu[AB]$, should decay to the $\pi[7^-]$ configuration. A possible explanation is that, because of the sharp backbend, the connection of the bands with the $\pi[7^-]$ configuration is lost. The $\Delta I = 1$ gamma-ray energies should jump from around 160 keV to 320 keV, and fall in a range of difficult observation, due to the presence of stronger discrete gamma rays from other bands. It is possible also that there is some delay in the connecting transitions, during which the recoiling nuclei might fly away from the center of the target chamber, therefore decreasing detection efficiency. The lower-spin states should be seen, though, from direct population, provided that the $\pi[7^-]$ band does not decay out easily, which we expect from K forbiddeness. Perhaps there is not enough direct population at these relatively low spins to make the band observable.

The values of the $M1/E2$ branching ratio as a function of frequency, calculated from the TAC model, are given in Figs. 6, 7, and 8. There is a reasonable agreement with the experimental data for the configurations proposed. However, from this agreement alone we cannot rule out the $\nu[h_{11/2}A]$ configuration for the bands in the even-even nuclei. Nevertheless, we believe this together with the moment of inertia behavior makes the proposed configurations more likely.

IV. TILTED AXIS CRANKING CALCULATIONS

The configuration assignments can be substantiated by tilted axis cranking (TAC) calculations, which study the interplay between rotational- and deformation-aligned angular momenta in a quantitative way providing both energies and in-band transition probabilities. The method is described in Refs. [1,2]. It has been recently applied to high-K bands in ^{163}Er [9], which seems to have some structural resemblance to ^{167}Yb. Details about the TAC calculations can be found in these references. Here we mention only some important features needed to understand the results. The rotational bands are associated with quasiparticle configurations in a potential that uniformly rotates about an axis tilted with respect to the principal axes of the deformed potential. The orientation is determined by minimizing the routhian (energy in the rotating frame) with respect to the tilting angle. For this equilibrium orientation the expectation value of the angular momentum $\vec{J}$ has the same direction as the cranking axis ($\vec{J} \parallel \vec{\omega}$). For the bands studied in this paper we assume axial symmetry which is a good approximation in this region (cf. [2]). The orientation is

TABLE II. Results of the tilted axis cranking model. The calculated tilting angle θ is given, together with the spin J, and its projection onto the symmetry axis J_3. The routhian e' is taken relative to the ground state band (g.s.) of ^{166}Yb. The reduced transition probabilities $B(M1)$ and $B(E2)$ are also given. The calculations were performed at a rotational frequency of $\omega = 0.25$ MeV.

Configuration	θ	$J(\hbar)$	$J_3(\hbar)$	e' (MeV)	$B(M1)$ (μ_N^2)	$B(E2)(e^2\,b^2)$
g.s.	90°	9.0	0.0	0.0	0.0	1.75
$\nu h_{11/2}$	44°	7.7	5.5	1.271	0.408	0.447
$\nu[h_{11/2}A]$	51°	12.9	8.2	1.13	0.474	0.657
$\pi[7^-]$	45°	10.5	7.4	0.876	0.564	0.470
$\pi[7^-]\otimes\nu[AB]$	64°	19.0	8.5	1.191	2.58	1.21
$\pi[7^-]\otimes\nu[AE]$	45°	18.2	12.8	1.171	0.553	0.626

fixed by the angle θ between the rotational axis and the symmetry axis (denoted by 3). In the calculations we use the deformation parameters $\epsilon_2 = 0.25$ and $\epsilon_4 = 0.01$. The pairing field is constant. The gap parameters are $\Delta_\pi = 0.91$ MeV and $\Delta_\nu = 0.86$ MeV. The proton and neutron chemical potentials are kept fixed and are chosen such that the expectation values are $Z \approx 70$ and $N \approx 97$ respectively at $\omega = 0$.

In the analysis of the experimental spectra it is useful to introduce the experimental angular velocity ω. In contrast to the standard cranked shell model (CSM) we operate with the total angular velocity instead of its projection onto the one-axis. The experimental frequency is simply equal to the γ-ray energy of the transition $I \to I - 1$ to which the angular momentum $J = I$ is assigned. The intraband transition probabilities are calculated from the TAC wave functions by means of the semiclassical expressions given in Refs. [1,2,11,9]. The results for $\omega = 0.25$ MeV are given in Table II.

Figure 11 shows the quasiparticle spectra in the TAC model. The lowest excitations are of quasineutron type. Since the collective rotation is about the one-axis (θ =

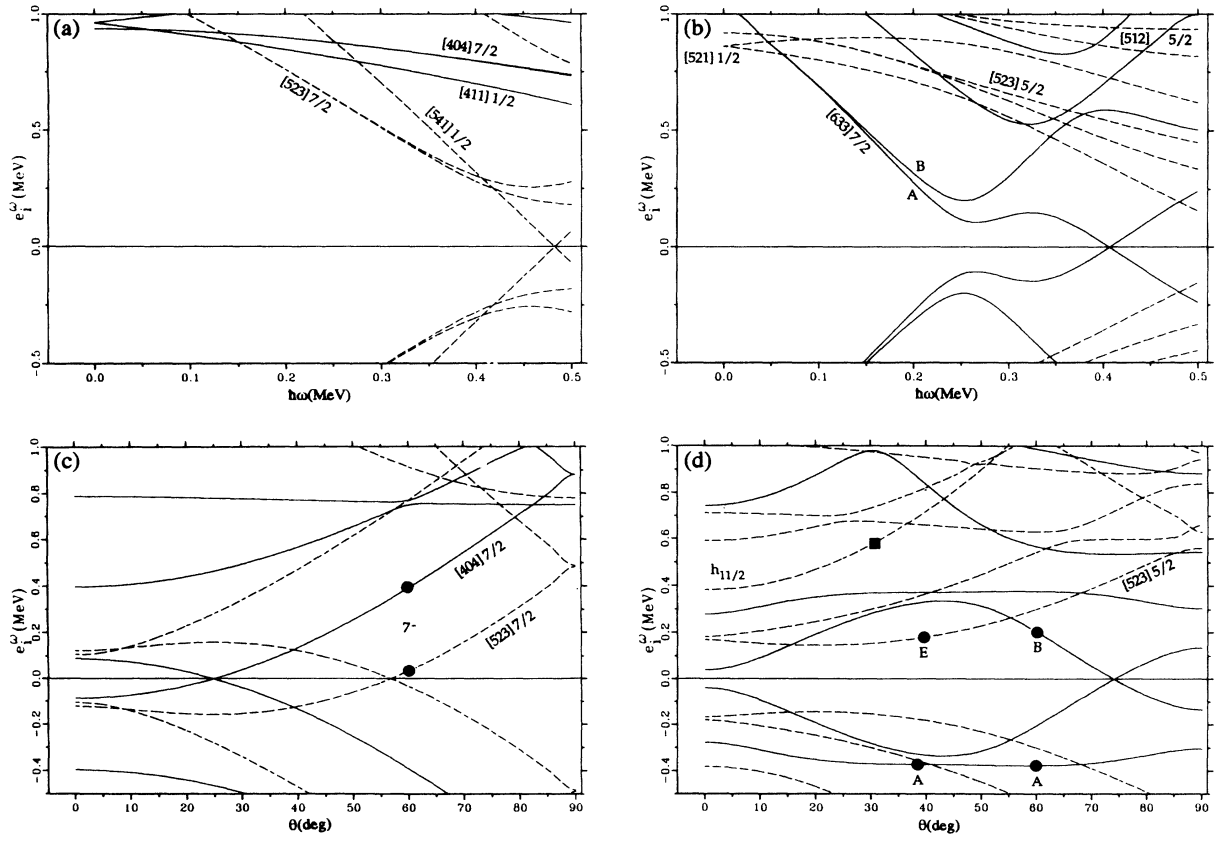

FIG. 11. Quasiparticle spectra for ^{166}Yb calculated from the TAC model. (a) Quasiproton routhians as a function of rotational frequency for $\theta = 90°$. (b) Quasineutron routhians as a function of rotational frequency for $\theta = 90°$. (c) Quasiproton routhians as a function of the tilting angle (θ) at $\hbar\omega = 0.3$ MeV. The circles indicate the occupation for the $\pi[7^-]$ configuration. (d) Quasineutron routhians as a function of the tilting angle (θ) at $\hbar\omega = 0.3$ MeV. The square indicates the occupation for the $\nu h_{11/2}$ configuration. The circles around $\theta = 60°$ and around $\theta = 38°$ indicate the occupations for the AB and AE configurations, respectively.

90°), the lowest quasineutron excitations are PAC (principal axis cranking) solutions with $\theta = 90°$. They form the lowest bands in ^{166,167,168}Yb, which can be classified as traditional CSM configurations with good signature quantum number [8,11]. An exception is the $h_{11/2}$ quasineutron orbit, which strongly slopes down towards $\theta = 0°$. It is a good example of strong coupling to the deformed potential, i.e., a DAL state in terms of the classification introduced in Ref. [12]. Figure 12(a) shows that at finite rotation the $h_{11/2}$ quasineutron has $i_3 \approx 5.5\hbar$ and a very small i_1 component. This is reflected by the routhian in Fig. 11(d), which is $e' \approx e'_0 - 5.5\hbar\omega\cos\theta$. The $h_{11/2}$ band observed in ^{167}Yb is assigned to this one quasineutron configuration. It is a TAC solution that represents what one is used to calling a high-K band. The component $J_3 = K$, the band starts at $I = K$, and all the angular momentum increase comes from the collective angular momentum R [cf. Fig. 12(a)] The tilting angle is to a good approximation given by the strong coupling expression

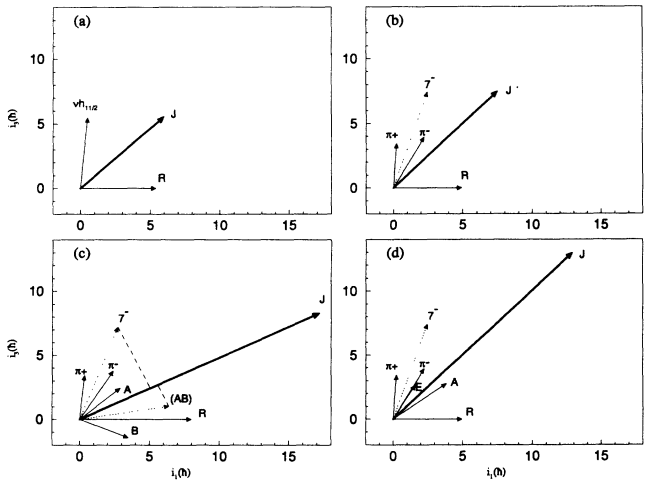

FIG. 12. Vector diagrams at $\hbar\omega = 0.25$ MeV. The thin solid line vectors represent the angular momentum of each quasiparticle, and the rotational angular momentum (R), which is parallel to the one-axis. The total spin (J) which is the vector addition of the quasiparticle and rotational angular momenta is indicated by a thick solid line vector. The angular momentum projections onto the one-axis is denoted by i_1 and onto the three-axis (the symmetry axis of the ellipsoid) by i_3. (a) Diagram for the $\nu h_{11/2}$ band. (b) Diagram for the $\pi[7^-]$ band. The dashed line vector is the vector addition of the two quasiprotons angular momenta. The positive parity quasiproton ($\pi[404]7/2^+$) is marked as π^+, and the negative parity one ($\pi[523]7/2^-$) as π^-. (c) Diagram for the $\pi[7^-] \otimes \nu[AB]$ band. The quasiproton angular momenta is indicated as in (b). The dashed line vector marked as (AB) is the vector addition of the two quasineutrons (A and B) angular momenta. The long-dashed lines represent the projection of the quasiproton and quasineutron angular momenta perpendicular to the total spin. Since the g factors of protons and neutrons have opposite signs, the magnetic moments add, yielding high $M1$ transition probabilities. (d) Diagram for the $\pi[7^-]\otimes\nu[AE]$ band. In this case the perpendicular component of the quasineutron angular momenta (A and E) is small.

$$\cos\theta = K/I, \quad I = \mathcal{J}\omega.$$

Figure 13 shows this behavior, which has the typical Hopf bifurcation [12] at the bandhead, which corresponds to the frequency $\omega_h = K/\mathcal{J}$ in the case of strong coupling. The calculated value $\hbar\omega_h = 0.198$ MeV is the lowest possible frequency for the $h_{11/2}$ band ($\theta = 0°$). As seen in Fig. 14, the calculations predict a back bend at $J = 15\hbar$ corresponding to the AB crossing in the $i_{13/2}$ quasineutron system. The presence of the $h_{11/2}$ quasineutron delays the AB crossing by $2\hbar$ as compared to the yrast line (shown in Fig. 14 as well). The experimental function $I(\omega)$ [Fig. 15(b)] does not show any irregularity up to I=33/2. Figure 10 seems to indicate a very smooth gain of moment of inertia that could be due to a very much smoothed out AB crossing. The systematic absence of the AB crossing in the $h_{11/2}$ quasineutron bands [9] is not fully understood at present. We performed also a $\Delta_\nu = 0$ calculation for this configuration. The corresponding $B(M1)/B(E2)$ is shown in Fig. 6. The experimental values lie more or less in between the $\Delta_\nu = 0$ and the full pairing calculation at the upper part of the band. Figure 15(a) shows also a $\Delta_\nu = 0$ calculation for the $\nu h_{11/2}$ band. Its spins are larger than for the full pairing calculation at the same frequency (the kinematic moment of inertia is larger), in agreement with the experimental trend. This indicates that pairing might be reduced for this configuration already at relatively low spins. This might explain the absence of the AB crossing in this band.

In the even-even isotopes both the neutron and proton excitations must be considered. The lowest two quasineutron excitations are the $(i_{13/2})^2$ configuration AB and the negative parity configuration AE, which are PAC solutions with $\theta = 90°$. They are the lowest bands. In Fig. 14 we show the g band and AB for reference. The combination of the $h_{11/2}$ quasineutron with the $i_{13/2}$ quasineutron A results in a TAC solution. Its tilting angle is shown in Fig. 13, its energy in Fig. 14, and spin in Fig. 15(a). It is one candidate for the observed $\Delta I = 1$ bands. As can be seen in Fig. 6, it has relatively small $B(M1)/B(E2)$ values, since the transversal magnetic moments of the two

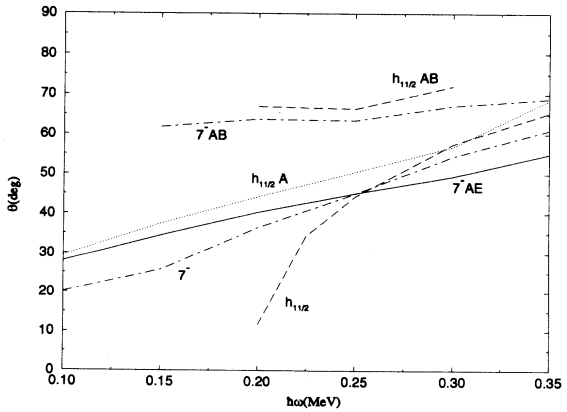

FIG. 13. Tilting angle as a function of rotational frequency. The configuration corresponding to each line is indicated in simplified notation (see text).

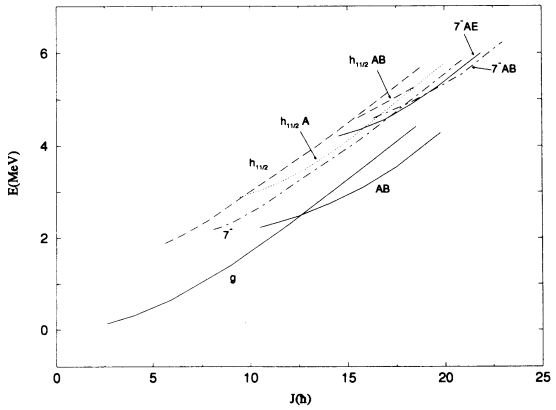

FIG. 14. Total energy (E) as a function of spin (J). The configurations are indicated as in Fig. 13.

quasineutrons cancel to a large extent.

Figure 11(c) shows that most of the quasiproton orbitals drive towards $\theta = 0°$, since they are relatively strongly coupled to the deformed field. For $\theta < 45°$ the orbitals coming from the Nilsson states [523]7/2 ($h_{11/2}$) and [404]7/2 are lowest. They combine into a two quasiproton configuration with $J_3 \approx 7$. For short notation we call it the 7^- configuration although its structure is more complicated than that of a simple K=7-band. As seen in Fig. 12(b), the $h_{11/2}$ quasiproton (π^-) is appreciably tilted away from the three-axis. Its energy minimum in Fig. 11(c) lies near $\theta = 30°$ indicating a character intermediate between DAL and FAL (Fermi-aligned) according to the classification scheme of Ref. [12]. The tilting takes place at the beginning of the band causing the relatively flat behavior of $\theta(\omega)$ at low ω in Fig. 13. The 7^- band has not been seen in the present experiment, but it is known in ^{164}Er [14].

For higher spin the 7^- two quasiproton configuration combines with quasineutron excitations. The lowest two quasineutron excitations are the configurations AB and AE coming from the corresponding PAC configurations at $\theta = 90°$ (cf. discussion above). However, the resulting four quasiparticle configuration is not just a simple combination of the 7^- with the AB and AE PAC bands. As can be seen from Fig. 11(d), the quasineutron orbits change noticeably with the orientation.

The orbital A has a minimum at $\theta = 45°$ qualifying it as a FAL quasineutron. Its energy does not depend very much on θ. It can follow the orientation of the rotational axis much better than other orbitals, since due to the reduction of its quadrupole moment by pairing it is only weakly coupled to the deformed field. The orbital B is RAL according to the classification in Ref. [12], since it has its minimum at $\theta = 90°$. It is responsible for the larger θ values in the configuration 7^-AB as compared with 7^- (cf. Fig. 13). This increase of θ and the contribution of B (negative g factor) to the transversal magnetic moment, which adds to the proton part, significantly enhance the $B(M1)$ values (cf. Fig. 7). This is illustrated in Fig. 12(c), which also demonstrates that A contributes only very little to the transversal magnetic moment. This is an example of the improvement brought

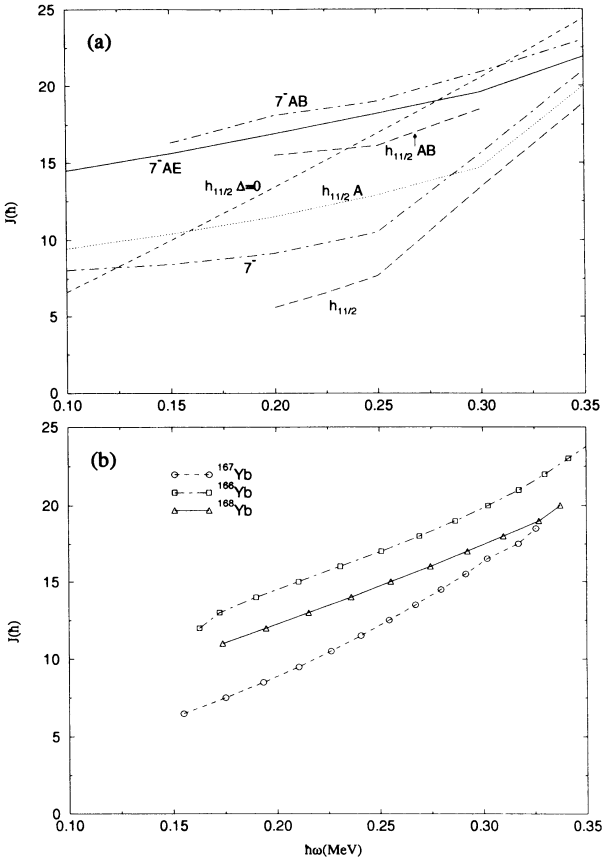

FIG. 15. Total angular momentum (J) as a function of rotational frequency. (a) TAC results. The configurations are indicated as in Fig. 13. (b) Experimental results. Circles ^{167}Yb ($\nu h_{11/2}$), squares ^{166}Yb (7^-AB, $I = 11$ assumed for the lowest-spin state), triangles ^{166}Yb (7^-AE, $I = 10$ assumed for the lowest-spin state). The experimental rotational frequency ($\hbar\omega$) of each state of spin J is the energy of the dipole γ-ray transition depopulating that state (see Fig. 5).

by the TAC calculation, when the simple estimates of the magnetic moments suggested in Ref. [10] are inaccurate (the three-component of A would not be included making its contribution much larger).

The E orbital changes its character with θ. At 90° it consists mainly of [521]1/2 having a routhian that is almost θ independent (as is characteristic of a $\tilde{\Lambda} = 0$ pseudospin state). Since they slope down with decreasing θ, orbits coming from Nilsson levels with larger K take over at lower θ. As a consequence, the quasineutron E contributes about $2.6\hbar$ to J_3 in the configuration 7^-AE, whereas lowest negative parity bands in ^{166,168}Yb (AE and AF) show a large signature splitting, characteristic for $J_3 \approx 0$ [7,8,11]. The $B(M1)$ values of 7^-AE are close to the ones of 7^-, since both A and E have small angles with the axis of rotation $\vec{J}$ [cf. Fig. 12(d)]. The large i_1 components of the quasineutrons A, B, and E make the tilting angle $\theta(\omega)$ much less spin dependent than would be expected from the strong coupling estimate (1). This is clearly seen in Fig. 13 when comparing the $h_{11/2}$ band with the other configurations.

The configurations 7^-AB, 7^-AE, and $\nu h_{11/2}A$ are

three candidates for the $\Delta I = 1$ sequences observed in ^{166,168}Yb. As seen in Fig. 14, we expect them to be close in energy. Our assignment to the 7^- quasiproton excitations is based on the slightly lower energy and the larger $B(M1)/B(E2)$ values compared to $\nu h_{11/2}A$. The assignment of 7^-AB to ^{166}Yb and of 7^-AE to ^{168}Yb relies on the evidence for an AB crossing in ^{166}Yb discussed in Sec. III. In view of the restricted information our data contain, these assignments must be considered as tentative.

V. SUMMARY AND CONCLUSIONS

Weakly populated high-K bands have been observed in the ^{166}Yb region. The properties of the bands observed for the first time in ^{166}Yb and ^{168}Yb have led to rather unusual tentative configuration assignments, i.e., $\pi[7^-]\otimes\nu[AB]$ and $\pi[7^-]\otimes\nu[AE]$, respectively. The tilted cranking model predicts lower excitation energies for such bands than would be expected from traditional models, and is able to reproduce the large $B(M1)/B(E2)$ ratios observed. Another possible configuration would be the $\nu[h_{11/2}\otimes i_{13/2}]$ for both bands in the even-even nuclei, which should present, however, lower $B(M1)/B(E2)$ ratios. The $\nu h_{11/2}$ band in ^{167}Yb has been extended to higher spins. A smooth increase in the dynamic moment of inertia as a function of spin is observed for this band up to $I = 33/2$. The presence or absence of the AB crossing in this band is not clear from the experimental data. The possibility of weaker pairing for this band is raised.

ACKNOWLEDGMENTS

This work was supported by the Director, Office of Energy Research, Division of Nuclear Physics of the Office of High Energy and Nuclear Physics of the U.S. Department of Energy under Contract No. DE-AC03-76SF00098 (LBL), and the U.S. Department of Energy under Contract No. W-7405-Eng. 48 (LLNL).

[1] S. Frauendorf, in *Proceedings of the International Symposium on Future Directions in Nuclear Physics with 4π Gamma Detection Systems of the New Generation*, Strasbourg, 1991, edited by J. Dudek and B. Haas, AIP Conf. Proc. No. 259 (AIP, New York, 1992), p. 223.
[2] S. Frauendorf, Nucl. Phys. **A557**, 259c (1993).
[3] K. Ya. Gromov *et al.*, Z. Phys. A **277**, 395 (1976).
[4] Th. Lindblad, Nucl. Phys. **A238**, 287 (1975).
[5] B. J. Meijer, F. W. N. De Boer, and P. F. A. Goudsmit, Nucl. Phys. **A259**, 213 (1976).
[6] R. Bengtsson and S. Frauendorf, Nucl. Phys. **A314**, 27 (1979).
[7] E. M. Beck, J. C. Bacelar, M. A. Deleplanque, R. M. Diamond, F. S. Stephens, J. E. Draper, B. Herskind, A. Holm, and P. O. Tjøm, Nucl. Phys. **A464**, 472 (1987).
[8] J. C. Bacelar, M. Diebel, C. Ellegaard, J. D. Garrett, G. B. Hagemann, B. Herskind, A. Holm, C.-X. Yang, J.-Y. Zhang, P. O. Tjøm, and J. C. Lisle, Nucl. Phys. **A442**, 509 (1985).
[9] A. Brokstedt, J. Lyttkens-Lindén, M. Bergström, L. P. Ekström, H. Ryde, J. C. Bacelar, J. D. Garrett, G. B. Hagemann, B. Herskind, F. R. May, P. O. Tjøm, and S. Frauendorf, Nucl. Phys. **A557**, 469c (1993); Nucl. Phys. **A571**, 337 (1994).
[10] F. Dönau and S. Frauendorf, in *Proceedings of the Conference on High Angular Momentum Properties of Nuclei*, Oak Ridge, Tennessee, 1982, edited by N. R. Johnson, Nucl. Sci. Res. Conf. Series No. 4 (Harwood, New York, 1983), p. 143.
[11] J. R. B. Oliveira, S. Frauendorf, M. A. Deleplanque, R. M. Diamond, F. S. Stephens, C. W. Beausang, J. E. Draper, C. Duyar, E. Rubel, J. A. Becker, E. A. Henry, and N. Roy, Phys. Rev. C **47**, R926 (1993).
[12] S. Frauendorf, Phys. Scr. **24**, 349 (1981).
[13] G. Jeschke, *Mathematik der Selbstorganisation* (Deutscher Verlag der Wissenschaften, Berlin, 1989), Chap. 6, p. 155.
[14] F. W. N. de Boer, P. F. A. Goudsmit, P. Koldewijn, and B. J. Mejer, Nucl. Phys. **A169**, 577 (1971).